Supplementary Information

O_v-rich γ-MnO_2 enhanced electrocatalytic three-electron oxygen reduction to hydroxyl radicals for sterilization in neutral media

Yingnan Qin [a], Tongzhu Han [b], Ligang Chen [*c], Kexin Yan [d], Jing Wang [e], Ning Wang [*a], Baorong Hou [a]

[a] Key Laboratory of Advanced Marine Materials, Key Laboratory of Marine Environmental Corrosion and Bio-fouling, Institute of Oceanology, Chinese Academy of Sciences, Qingdao, 266071, China

[b] Marine Bioresource and Environment Research Center, Key Laboratory of Marine Eco-Environmental Science and Technology, First Institute of Oceanography, Ministry of Natural Resources, Qingdao, 266061, China

[c] State Power Investment Corporation Hydrogen Energy Company, Limited, Beijing 102600, China

[d] College of Environmental and Safety Engineering, Qingdao University of Science and Technology, Qingdao 266042, PR China

[e] College of Chemical Engineering, Qingdao University of Science and Technology, Qingdao 266042, PR China

Electrochemical measurements.

All the electrochemical tests were conducted on CS2350M electrochemical workstation (Wuhan Corrtest Instrument Co., LTD). Before electrochemical measurements, 5 mg of as-prepared catalysts were dispersed in 1 mL mixture of DI water, ethanol, and 5 wt% Nafion solution (volume ratio is 1: 1: 0.0001) to form a uniform ink. All the electrochemical measurements were conducted in a three-electrode system, with a catalyst-modified RRDE as working electrode, saturated calomel electrode (SCE) as reference electrode, and carbon rod as counter electrode. 10 μL ink was dropped onto the glassy carbon disk electrode of RRDE, and rotary drying under the ambient environment. Cyclic voltammetry was conducted in N_2-saturated 3.5 wt% NaCl solution at a potential range of 0-1.2 V *vs.* RHE, with a scan rate of 500 mV/s for 50 cycles, to get a stable curve. The linear polarization curve (LSV) was measured at 0-1.1 V *vs.* RHE with a scan rate of 20 mV/s and a rotate speed of 1600 rpm. The RRDE tests were performed in an O_2-saturated solution with a scan rate of 20 mV/s and rotate speed of 1600 rpm, with the ring potential was fixed at 1.2 V *vs.* RHE. The selectivity of H_2O_2 (H_2O_2%) via $2e^-$ ORR pathway and the number of transfer-electron (n) can be calculated by the following equation based on the disk current (I_D) and ring current (I_R) measured by RRDE.

$$H_2O_2\%\ (\%) = \frac{200 \times I_R/N}{|I_D| + I_R/N} \quad (S1)$$

$$n = \frac{4 \times |I_D|}{|I_D| + I_R/N} \quad (S2)$$

Here, N refers to the collection coefficient of RRDE, which depends on only the size of RRDE and is 37% in this system.

H_2O_2 yield tests.

The tests of H_2O_2 yield were conducted in a traditional three-electrode system with catalyst-loaded carbon paper (mass loading: 0.2 mg cm^{-2}) as working electrode, saturated calomel electrode as reference electrode, and graphite rod as counter electrode. All the tests were performed in 35 mL O_2-satureted 3.5 wt% NaCl solution at 0.1 V (*vs.* RHE) for 2 h in a separate chamber with Nafion 117 as the membrane. The concentration of H_2O_2 was measured using the cerium sulfate titration method based on

the color variation with Ce^{4+} concentration as described in Eq. S3. The Ce^{4+} concentration-absorbance standard curve was plotted by UV-visible adsorption peak at 318 nm for a range of Ce^{4+} solutions, and the final correction curve was $y = -0.015 + 5.21x$ (y is UV-visible absorbance, x is the concentration of Ce^{4+}). The electrolyte after i-t test was mixed with 0.5 mM $Ce(SO_4)_2$ solution at a volume ratio of 1: 49, and reacted for another 2 h, and the corresponding H_2O_2 concentration ($c_{H_2O_2}$) was calculated by Eq. S4. Finally, the H_2O_2 yield was calculated by Eq. S5.

$$2Ce^{4+}(yellow) + H_2O_2 \longrightarrow 2Ce^{3+}(colorless) + 2H^+ + O_2 \uparrow \quad (S3)$$

$$c_{H_2O_2}\ (mM) = \frac{(c_0 - x)/2}{1/50} \quad (S4)$$

Where the c_0 is the original Ce^{4+} standard solution with a concentration of 0.5 mM.

$$H_2O_2\ yield\ rate\ (mmol\ g_{cat}^{-1}\ h^{-1}) = \frac{c_{H_2O_2} \cdot v}{t \cdot m_{cat}} \quad (S5)$$

Where v is the volume of electrolyte (35 mL), t is reaction time (2 h), and m_{cat} is the loading mass of as-prepared catalysts (0.2 μg cm^{-2}).

Conditions of on-line SPE LC-MS/MS system.

Salicylic acid in samples was concentrated and detected by the on-line SPE-LC-MS/MS system, which was carried out on a 1290 II ultrahigh-performance liquid chromatography coupled with a 6470 triple quadrupole mass spectrometry system (Agilent, Santa Clara, CA, USA). A schematic of the online SPE-LC-MS/MS is presented in **Fig. S1.** The online SPE system consists of a high-performance (with a 900 μL sample loop), a quaternary pump (P1), binary pump (P2) and a thermostatic column compartment equipped with a six-port valve. Chromatographic separation was performed on a Zorbax Extend C18 (3.5 μm, 3.0 mm × 150 mm) from Agilent (Santa Clara, CA, USA). A guard column Zorbax Eclipse XDB-C8 (5 μm, 2.1 mm × 12.5 mm) from Agilent was employed as a trap column for the online SPE. Details of on-line SPE-LC-MS/MS conditions are listed in **Table S1 and S2**.

DFT calculation.

All density functional theory (DFT) calculations carried out on the $MnO_2(O_v)$ and $Mn_3O_4(O_v)$ catalysts were performed via Vienna ab initio simulation package (VASP) with the projector augmented wave (PAW) method[1]. The generalized gradient

approximation (GGA) with the Perdew-Burke-Ernzerhof (PBE) was adopted to describe the exchange-correlation functional[2]. The DFT-D3 method is used to introduce van der Waals (vdW) interaction. Spin polarization was considered in the calculation[3]. The U parameter of the Mn atom is set to 4 eV[4]. The kinetic energy cutoff was set to 400 eV, and the force and energy convergence criteria were set to 0.03 eV/Å and 10^{-4} eV, respectively.

A slab model of MnO_2 with (300) crystal faces consisting of 16 Mn atoms and 32 O atoms was constructed using an optimized MnO_2 single cell. A slab model of Mn_3O_4 with (101) crystal faces consisting of 28 Mn atoms and 48 O atoms was constructed using an optimized Mn_3O_4 single cell. The vacuum layer of the slab model for MnO_2 and Mn_3O_4 is set to 20 Å. $MnO_2(O_v)$ and $Mn_3O_4(O_v)$ slab models with oxygen vacancies are constructed by removing one oxygen atom from the surface of the MnO_2 and Mn_3O_4 slab models. For geometric optimization, the bottom two atomic layers of all slab models are fixed, and the upper atomic layers remain relaxed.

The adsorption energy of O_2 molecules at active sites on the catalyst surface was calculated by the following equation:

$$\Delta E_{*O_2} = E_{*O_2} - E_* - E_{O_2}$$

Where * refers to O_v-γ-MnO_2 or O_v-Mn_3O_4. E_{*O_2} refer to the total energy after the adsorption of O_2 on the catalyst surface. E_* is the total energy of the catalyst. E_{O_2} refer to the energy of O_2 molecules.

During the calculation of the reaction mechanism, Gibbs free energy (G) was obtained by the following equation:

$$\mathrm{G} = \mathrm{E} + \mathrm{ZPE} - \mathrm{TS}$$

Where E, ZPE and TS were total energy, zero-point energy and entropic contributions, respectively. ZPE and TS were processed by the vaspkit code at 298.15 K[5].

Antibacterial performance tests.

Pseudomonas aeruginosa (*P. aeruginosa*) and staphylococcus aureus (*S. aureus*) were used as the typical strain to invest the antibacterial performance of as-prepared catalysts. First of all, the typical strains were cultured in LB medium, after 12 h preservation at

37°C, the bacteria body was centrifugated at 4000 rpm for 5 min, and redispersed in 0.1 M phosphate buffer saline (PSB) to get a uniform solution with a concentration of 10^7 cfu/mL. The antibacterial test was carried in 35 mL above solution, with catalyst-modified carbon paper (1×2 cm, with a loading mass of 0.2 mg/cm^2) as working electrode, SCE as reference electrode, and carbon rod as counter electrode. Electrolytes were collected after 0, 10, 30, 60, 120, and 180 min chronoamperometry test with an applied potential at 0.1 V *vs.* RHE. Coating the above electrolytes onto nutrient agar medium plates, keeping at 37°C for 24 h, counting the colony number of each plate and calculating the disinfection rate with the variation of time.

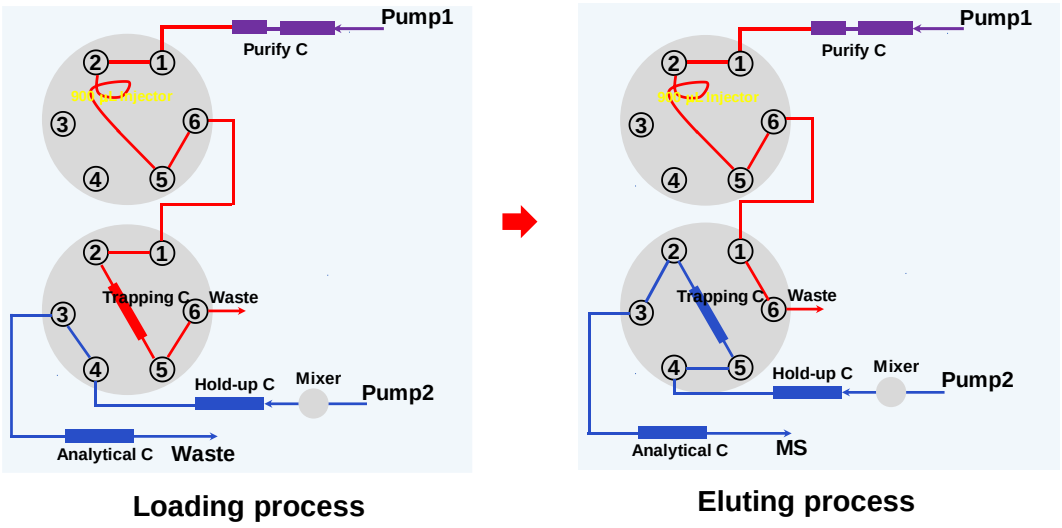

Figure S1 Schematic of the online SPE-LC-MS/MS.

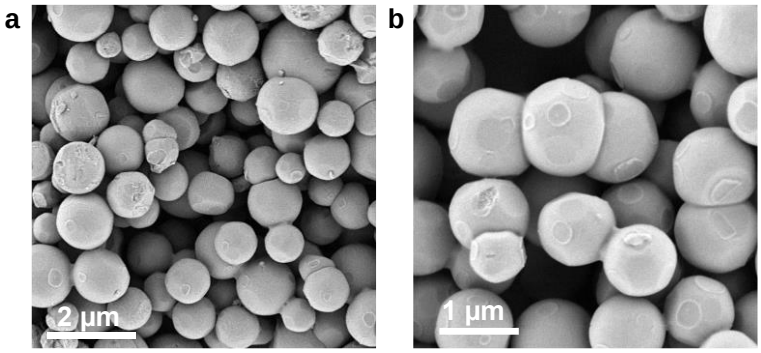

Figure S2 SEM images of PBA precursor.

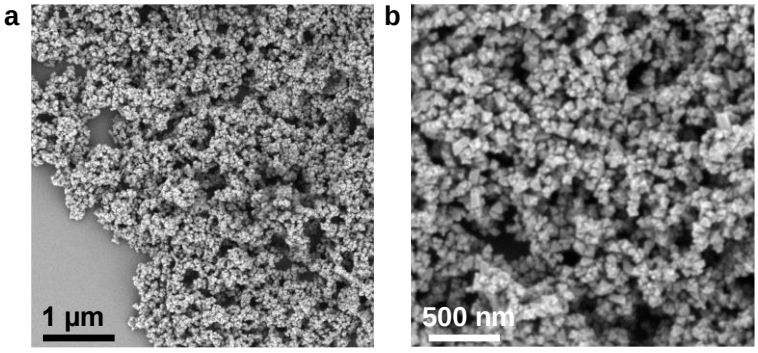

Figure S3 SEM images of ammonia-treated PBA.

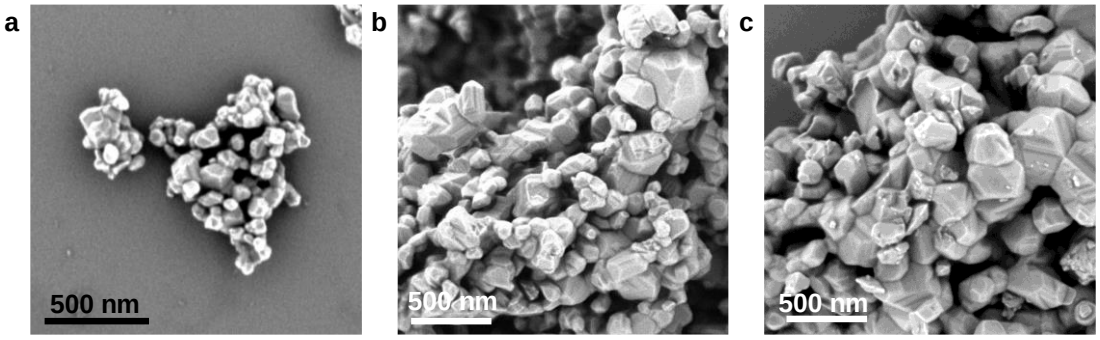

Figure S4 SEM images of Mn_3O_4-x with different calcination temperature. (**a**) Mn_3O_4-700, (**b**) Mn_3O_4-800, (**c**) Mn_3O_4-900.

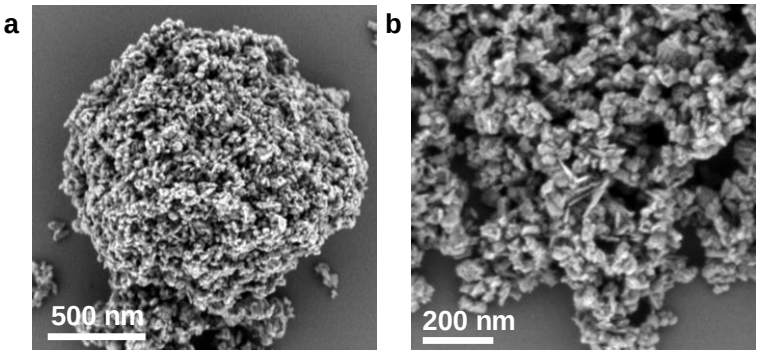

Figure S5 SEM images of MnO_2-700A

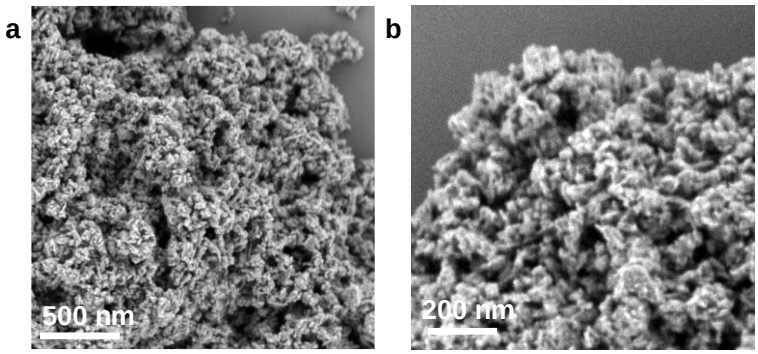

Figure S6 SEM images of MnO_2-800A

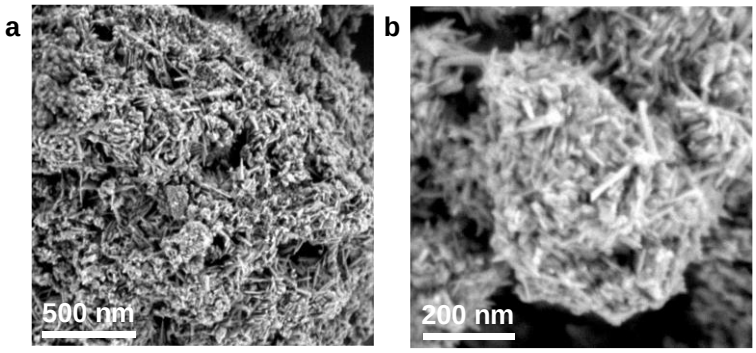

Figure S7 SEM images of MnO_2-900A

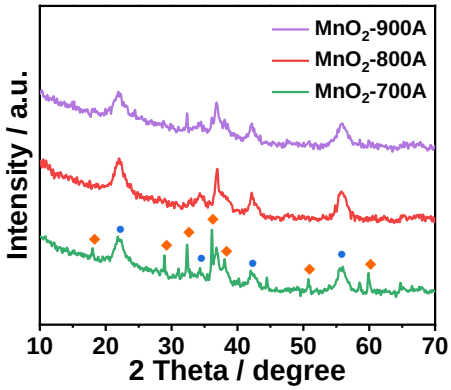

Figure S8 XRD patterns of as-prepared MnO_2-xA catalysts.

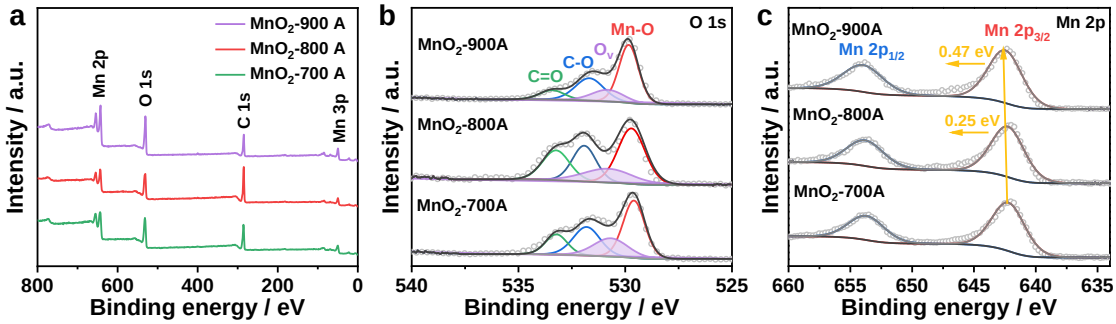

Figure S9 XPS patterns of as-prepared MnO_2-xA catalysts. (**a**) survey-scan spectra, (**b**) O 1s spectra, (**c**) Mn 2p spectra.

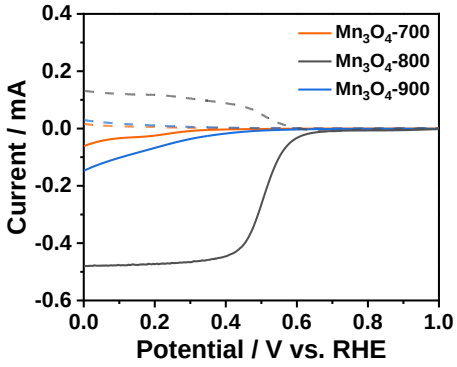

Figure S10 RRDE polarization curves of Mn_3O_4-x.

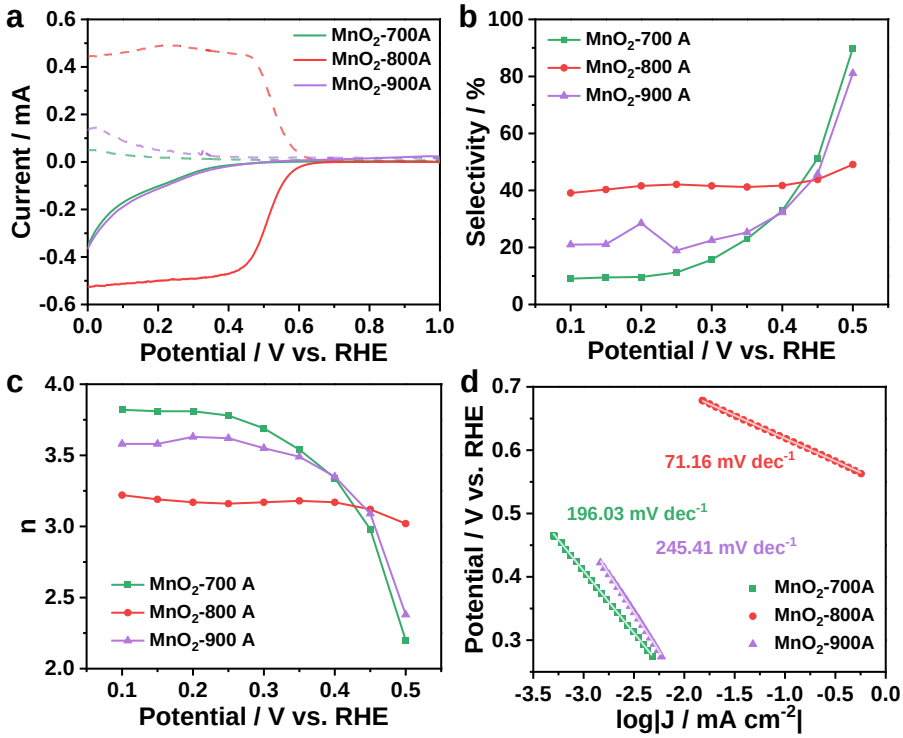

Figure S11 Electrochemical performance of as-prepared MnO_2-xA catalysts. (**a**) RRDE polarization curves, (**b**) H_2O_2 selectivity, (**c**) number of transfer electron, (**d**) Tafel curves.

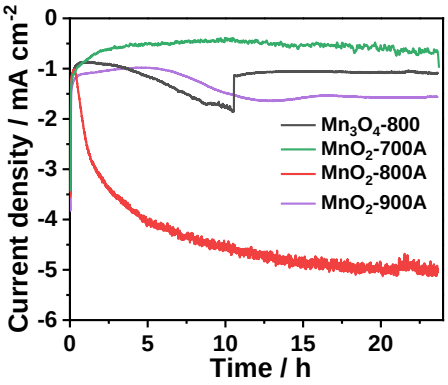

Figure R12 The stability of as-prepared catalysts.

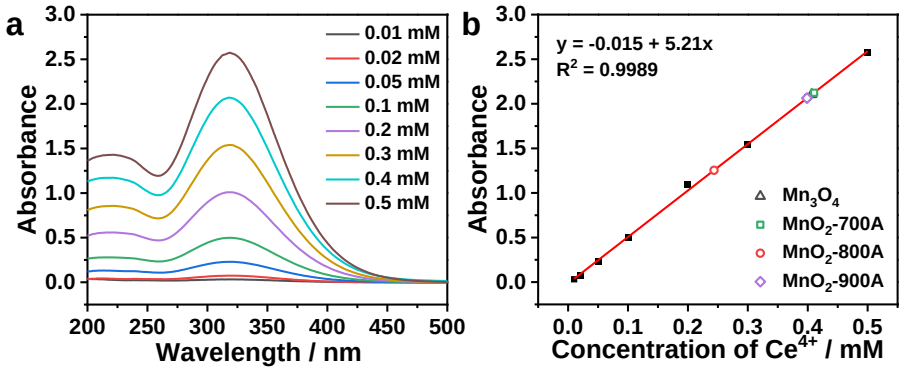

Figure 13 (**a**) UV-visible spectra of $CeSO_4$ at various concentrations, (**b**) calibration curve of the absorbance and Ce^{4+} concentration at 318 nm.

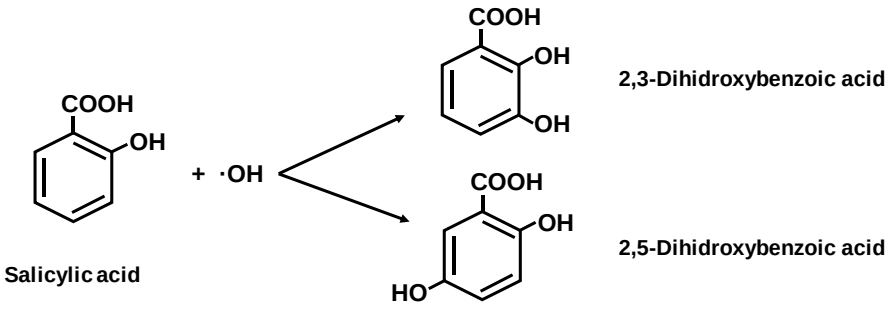

Figure S14 The equation of the reaction of salicylic acid and hydroxyl radical.

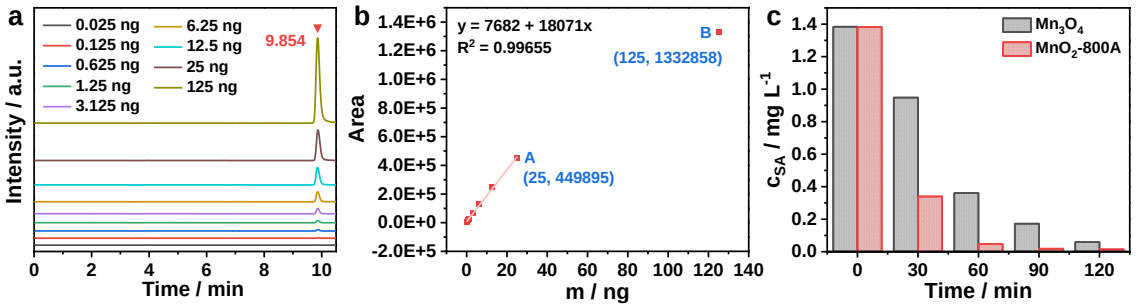

Figure S15 (**a**) curves of LC-MS/MS for salicylic acid at different masses, (**b**) calibration curve of the peak area and mass of salicylic acid, (**c**) variation of salicylic acid concentration with different reaction times.

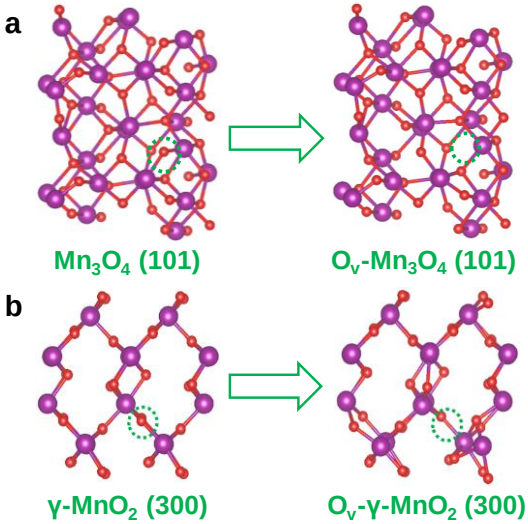

Figure S16 The configurations of (**a**) Mn_3O_4 (101), O_v-Mn_3O_4 (101), (**b**) γ-MnO_2 (300) and O_v-γ-MnO_2 (300) models.

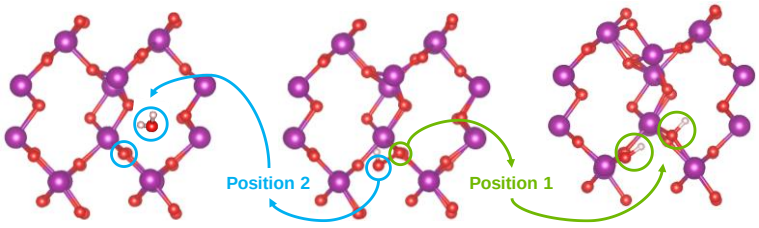

Figure S17 The O position on adsorbed *OOH in O_v-γ-MnO_2 (300).

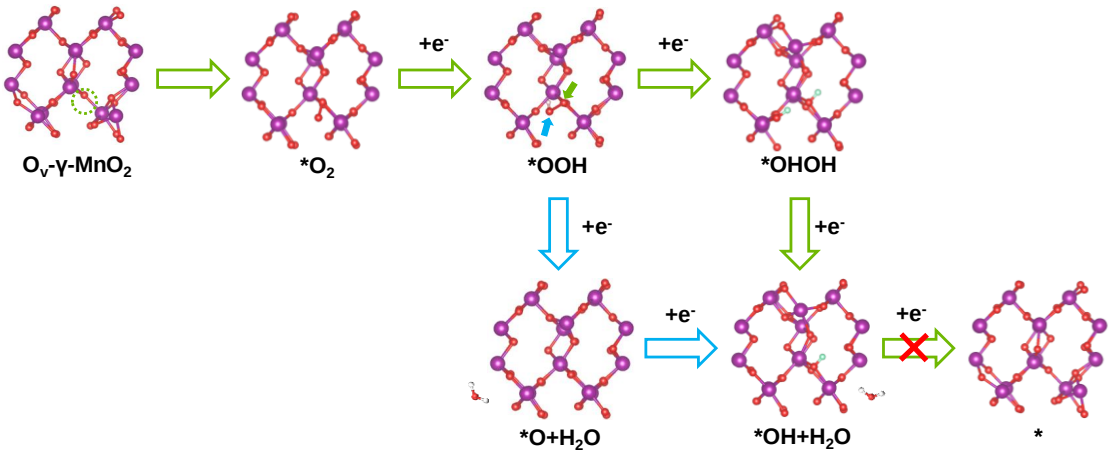

Figure S18 Geometry adsorption configurations of $3e^-$ ORR progress on O_v-γ-MnO_2 (300).

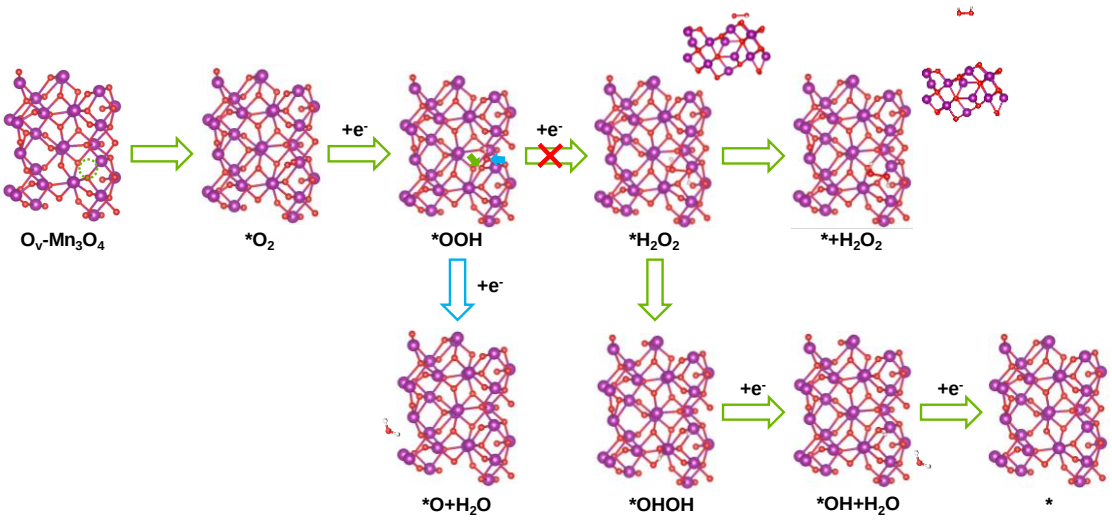

Figure S19 Geometry adsorption configurations of $3e^-$ ORR progress on O_v-Mn_3O_4 (101).

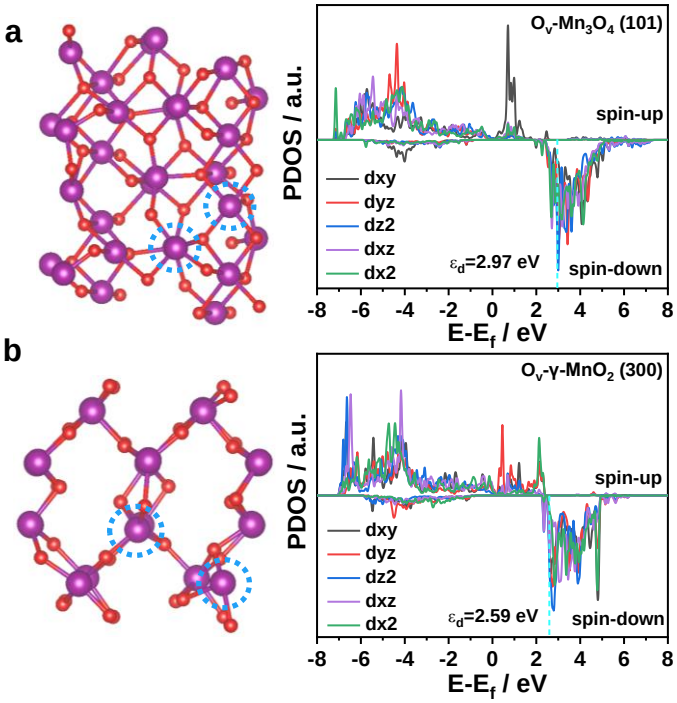

Figure S20 The projected density of state (PDOS) analysis. (**a**) O_v-Mn_3O_4 (101) and (**b**) O_v-γ-MnO_2 (300). (The two Mn atoms in the blue dotted circles are the active sites of as-prepared catalysts, all the PDOS and d-band center analysis are based on that.)

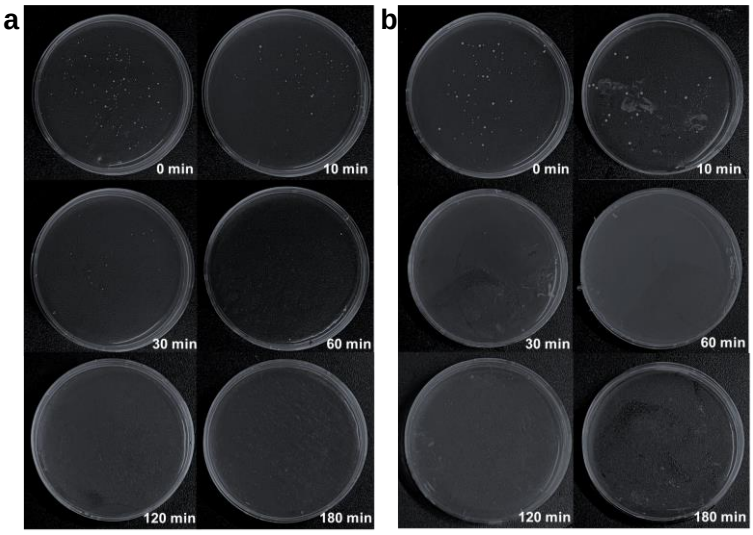

Figure S21 Digital pictures of colony plates with different reaction times without the addition of IPA. (**a**) *P. aeruginosa*, (**b**) *S. aureus*.

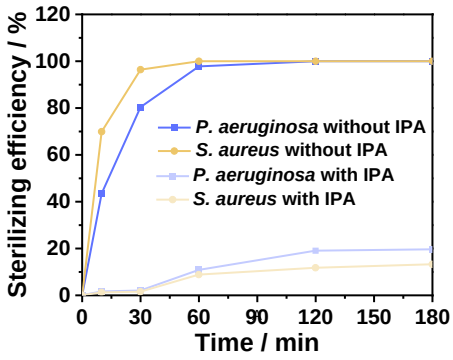

Figure S22 Variety of sterilization efficiencies for different reaction times.

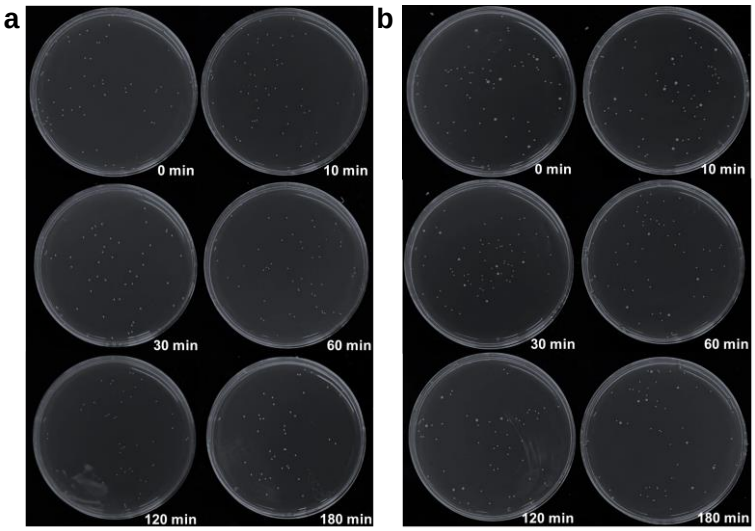

Figure S23 Digital pictures of colony plates with different reaction times with the addition of IPA. (**a**) *P. aeruginosa*, (**b**) *S. aureus*.

Table S1. LC parameters and MS/MS parameters of the instrumental method for Salicylic acid analysis.

LC parameters					
Instrument	HPLC 1260 and UPLC 1290 (Agilent Technologies, USA)				
Analytical column	Zorbax Extend C18, 3.5 μm, 3.0 mm × 150 mm (Agilent Technologies, USA)				
Trapping column	Zorbax Eclipse XDB-C8, 5 μm, 2.1 mm × 12.5 mm (Agilent Technologies, USA)				
Injection volume	100 μL (Needle rinsed once with 1:1 methanol: water before injection)				
Column temperature	30 °C				
Mobile phases UP 1290	Flow rate: 0.3 mL min^{-1} A1: Ultrapure water with 0.5% formic acid B1: Methanol				
Mobile phases HP 1260	A: Ultrapure water with 0.5% formic acid B: Methanol				
Gradient UP 1290	Time / min	A / %	B / %		note
	0.0	80	20		equilibration
	2.0	80	20		
	7.0	50	50		
	10.5	0	100		
HP 1260	Time / min	Flow rate / mL min^{-1}	A / %	B / %	note
	0	0.5	95	0	loading
	2	0.5	95	0	
	10.5	0.5	95	0	equilibration
MS/MS parameters					
Instrument	6470 triple quadrupole mass spectrometer (Agilent				

	Technologies, USA)
Ion source	Agilent Jet stream (Agilent Technologies, USA)
Ionization	Electrospray ionization (ESI) in negative mode
Gas temp	300 ℃
Gas flow	3 L/min
Nebulizer	5 psi
Sheath gas temp	350 ℃
Sheath gas flow	7 L/min
Capillary voltage	3500 V
Scan type	MS2 SIM

Table S2. Retention times, molecular formula (precursor ion), monitored mass, fragmentor, collision energy.

Acronym analyte	Retention Time /min	Molecular formula	Monitored mass / m/z	Fragmentor / V	Collision energy / V
SA	9.85	$[C_7H_6O_3]^-$	137	100	5

Table S3 Binding energy and ΔE of as-prepared catalysts in Mn 3s XPS spectra.

	Binding energy / eV	ΔE /eV
Mn_3O_4-800	88.59 / 83.08	5.51
MnO_2-700A	89.05 / 84.23	4.82
MnO_2-800A	88.76 / 83.99	4.77
MnO_2-900A	88.78 / 83.94	4.84

Table S4 Percentage of O with different configuration of as-prepared catalysts in O 1s spectra.

	Mn-O	O_v	C-O	C=O
Mn_3O_4-800	55.4	26.5	9.4	8.7

MnO_2-700A	38.8	19.4	12.2	29.6
MnO_2-800A	39.1	17.6	22.2	21.1
MnO_2-900A	47.9	15.5	26.7	9.9

Table S5 The peak intensity of UV-visible spectrum and the corresponding Ce^{4+} concentration, the amount of H_2O_2 and its yield rate after 2 h i-t tests.

	Peak intensity	c_{Ce4+} / mM	n_{H2O2} / mmol	H_2O_2 yield rate / mmol g^{-1} h^{-1}
Mn_3O_4-800	2.10	0.406	82.25	205.63
MnO_2-700A	2.12	0.401	78.75	196.88
MnO_2-800A	1.25	0.243	224..88	562.19
MnO_2-900A	2.06	0.398	89.25	223.13

Table S6 The peak area of HPLC curve and the corresponding SA mass and ·OH concentration.

Reaction	Mn_3O_4			MnO_2-800A		
Time / min	Peak area	m_{SA} / ng	$C_{\cdot OH}$ / mg L^{-1}	Peak area	m_{SA} / ng	$C_{\cdot OH}$ / mg L^{-1}
0	1475942	138.42	0	1475896	138.42	0
30	1010819	94.80	0.436	611287	33.97	1.044
60	649961	36.12	1.023	91899	4.66	1.337
90	319297	17.24	1.211	40791	1.83	1.336
120	115031	5.94	1.325	33923	1.45	1.369

Table S7 $3e^-$ ORR performance comparison between different catalysts.

Sample	H_2O_2 yield	·OH yield	Application	Ref.
OCNT	12 mg L^{-1} cm^{-1}		97.05 % of STZ degradation efficiency in 180 min	[6]

Cu/$CoSe_2$/C			98% of CIP degradation efficiency in 60 min	[7]
TiO_2/C cathode		2.69 μg cm^{-2} min^{-1}		[8]
FeCoC	1350 ± 38.9 μM/2 h		100.0 % removal of CIP in 5 min	[9]
1.0-MnCu/C			94.7% removal of TCH in 60 min	[10]
$FeCl_2C_x$/PC		48.86 μM t	98.12% removal of AMX in 15 min	[11]
MnO_2-800A	562.2 mmol g_{cat}^{-1} h^{-1}	2.09 mg L^{-1} h^{-1}	97.8% sterilization efficiency of *P. aeruginosa* in 60 min; 96.4% sterilization efficiency of *S. aureus* in 30 min	This work

References:

1. G. Kresse, *Physical Review B* 1996, **54**, 11169-11186.
2. K. B. John P. Perdew, Matthias Ernzerhof, *Phys. Rev. Lett.*, 1996, **77**, 3865-3868.
3. S. Grimme, *J. Comput. Chem.*, 2006, **27**, 1787-1799.
4. Z. Shi, Y. Wang, J. Li, X. Wang, Y. Wang, Y. Li, W. Xu, Z. Jiang, C. Liu, W. Xing and J. Ge, *Joule*, 2021, **5**, 2164-2176.
5. V. Wang, N. Xu, J.-C. Liu, G. Tang and W.-T. Geng, *Comput. Phys. Commun.*, 2021, **267**, 108033.
6. J. Zhang, S. Qiu and F. Deng, *J. Hazard. Mater.*, 2024, **465**, 133261.
7. L. Xie, P. Wang, W. Zheng, S. Zhan, Y. Xia, Y. Liu, W. Yang and Y. Li, *Proc. Natl. Acad. Sci. U. S. A.*, 2023, **120**, e2307989120.
8. F. Miao, M. Gao, X. Yu, P. Xiao, M. Wang, Y. Wang, S. Wang and X. Wang, *Electrochem. Commun.*, 2020, **113**, 106687.
9. F. Xiao, Z. Wang, J. Fan, T. Majima, H. Zhao and G. Zhao, *Angew. Chem. Int. Ed.*, 2021, **60**, 10375-10383.
10. D. Shang, S. Wang, J. Li, S. Zhan, W. Hu and Y. Li, *Small*, 2024, 2311984.
11. R. Ren, X. Shang, Z. Song, C. Li, Z. Wang, F. Qi, A. Ikhlaq, J. Kumirska, E. Maria Siedlecka and O. Ismailova, *Chem. Eng. J.*, 2023, **474**, 145545.